Preparation of Multinuclear Microparticles Using a Polymerization in Emulsion Process

F. Salaün,[1] E. Devaux,[1] S. Bourbigot,[2] P. Rumeau[3]

[1]*Laboratoire de Génie et Matériaux Textiles (GEMTEX), UPRES EA2461, Ecole Nationale Supérieure des Arts et Industries Textiles (ENSAIT), BP 30329, 59056 Roubaix Cedex 01, France*
[2]*Procédés d'Élaboration des Revêtements Fonctionnels (PERF), LSPES UMR-CNRS 8008, École Nationale Supérieure de Chimie de Lille (ENSCL), BP 90108, 59652 Villeneuve d'Ascq Cedex, France*
[3]*Institut Français du Textile et de l'Habillement, Direction Régionale Rhône-Alpes PACA, Avenue Guy de Collongue, 69134 ECULLY Cedex, France*

Received 12 January 2007; accepted 22 August 2007
DOI 10.1002/app.27283
Published online 9 November 2007 in Wiley InterScience (www.interscience.wiley.com).

ABSTRACT: A new microencapsulation method, in which a paraffin medium and small sub-micron spheres were encapsulated by an amino resin has been established. These multinuclear microparticles were made by polymerization in emulsion and characterized by scanning electron microscopy and interfacial tension measurements. This process is based on several emulsion mixings following Torza and Mason's approach, in which we combined the characteristics of a coacervation with a conventional interfacial reaction and an *in situ* polymerization followed by a water in oil in water emulsion. The inner phase of the microcapsules consisted of a mixture of paraffin and microspheres of poly(vinyl) alcohol/hydrated salt crosslinked by methylene diisocyanate. The encapsulation mechanism is based on the liquid/solid–liquid separation of methoxylolmelamines and will be described in this study to explain the surface morphology. © 2007 Wiley Periodicals, Inc. J Appl Polym Sci 107: 2444–2452, 2008

Key words: core-shell polymers; crosslinking; emulsion polymerization; microgels; microencapsulation

INTRODUCTION

The synthesis of composite polymer microcapsules including an inorganic component has attracted considerable attention due the combination of the properties of an inorganic nanoparticle with those of the polymeric system in an advantageous way, e.g., merging the thermal stability, the mechanical strength of the inorganic nanoparticle with the elasticity and the ability of the polymer to form coating. This latter could prevent their aggregation in liquids and improve their chemical stability. Various techniques for the fabrication of hybrid organic/inorganic capsules have been explored to obtain the required properties. The processes used are based on the sol-gel process[1] or the microemulsion technique[2] to form inorganic particles and emulsion or miniemulsion polymerization[3] for the preparation of polymer particles.

The morphology of the particles is crucial for achieving the desired properties. The structure of these particles depends on the choice of the polymers that entrap the core material and the synthesis parameters such as the type of organic solvent or solvent mixture used, the phase ratio of the emulsion system, the temperature, the type and the concentration of surfactants.

One of the trend of these two past decades is microencapsulated phase change materials (PCMs), which provide enhanced thermal insulation in a wide variety of applications. Microencapsulation of these organic materials have been widely studied, and numerous chemical and physical techniques based on coacervation and interfacial polymerization have been reported.[4–10] Nevertheless, these process are often limited by the use of organic PCMs and do not offer the possibility to merge the thermal properties with an inorganic compound.

The method presented here leads to microparticles with a double polymeric shell containing nanospheres and PCMs. The outer membrane is a three-dimensionnal crosslinked system obtained by an *in situ* polymerization of melamine-formol resin, whereas the inner part corresponds to occluded nanoparticles crosslinked by aminoplast bridges. The formation of a new skin layer is necessary to introduce new functions, especially to improve the thermal properties of the microparticles in comparison with PCM and microcapsules containing PCMs. Their morphology will be discussed in the study using the approach of Torza and Mason[11] based on interfacial spreading, which remains valid even if one of the phases is solid (the polymeric shell).[12,13]

Correspondence to: F. Salaün (fabien.salaun@ensait.fr).

TABLE I
Relationships Between the HLB Ratio of a Span® 85/Dioleate PEG 400 Mixture, the Emulsion Type, Stability and Particle Size Distribution

HLB of surfactants	Emulsion		
Span® 85/Dioleate PEG 400 (wt %/wt %)	Type	Stability[a]	Mean diameter[b] (μm ± SD)
2 (97/3)	Undefined	−	9.59 ± 12.66
3 (81.5/18.5)	w/o	+	6.85 ± 5.03
4 (66/34)	w/o	+	1.98 ± 1.33
5 (50.8/49.2)	w/o	++	1.66 ± 1.02
6 (35.4/64.6)	w/o	+++	1.58 ± 0.86
7 (20/80)	w/o	+	2.62 ± 1.63
8 (5/95)	o/w/o	−	15.68 ± 10.84

[a] Classification: +++, excellent; ++, good; +, satisfactory; −, poor.
[b] Particle diameters were obtained with a laser-light blocking technique (Accusizer TM, model 770, Particle sizing systems, Santa Barbara, CA, and C770 software version 2.54).

The originality of the system described in this article lies on the chemical nature of the PCMs, which are an inorganic salt entrapped in the nanoparticules and a paraffin as engulfing medium. This latter plays two main roles in the first step of the synthesis, e.g., the role of solvent and suppress Ostwald ripening of the salt droplet since it is an hydrophobic compound.[14]

EXPERIMENTAL

Materials

Disodium hydrogen phosphate dodecahydrate, Na_2HPO_4, $12H_2O$ (DSP) (ACROS Organics) was used as core material. Poly(vinyl alcohol) (PVA) 95% hydrolyzed (M_w = 95,000) from Acros Organics was used as film-forming materials (the coacervant agent is DSP). The crosslinking of PVA was carried out using a diisocyanate monomer. Diphenyl methylene diisocyanate (MDI) (Suprasec 2030, Hüntsman ICI; blend of MDI isomers, 4,4′-diphenyl methylene diisocyanate principally) was kindly dupplied by Hüntsman ICI.

n-Hexadecane (C_{16}) was purchased from Aldrich, with purity grade of 99.4% and the majority impurity is C_{15} (0.35%) was employed as lipophilic phase without purification before encapsulation by a melamine-formaldehyde hexamethylolated (Arkofix NM) kindly supplied by Clariant (France).

Polyoxyethylene (20) sorbitan monolaurate (i.e., Tween® 20 or Tw-20), obtained from Acros Organics, and sorbitan trioleate (i.e., Span® 85 or Sp-85), poly(ethylene glycol) dioleate (PEG 400 dioleate) purchased from Aldrich, were used as surfactants.

Synthesis of the multinuclear microparticles

Preparation of PVA-MDI microspheres

About 4 g of DSP and 2 g of water were mixed and added to a solution of 0.5 g of mixture of nonionic surfactants in 7 g of *n*-hexadecane. The different compositions of the surfactants used are listed in Table I. After stirring during 15 min, the droplet size was reduced by homogenizing the emulsion during 15 min at 9500 rpm with an Ultra-Turrax homogenizer (Ika, Germany). In the same way, another emulsion was prepared by homogenizing 8 g of PVA solution (5 wt %) in 8 g of *n*-hexadecane. The microspheres were prepared by shearing under high speed the two emulsions (emulsions 1 and 2) with 3 g of MDI to crosslink the shell at 50°C for 30 min. The method used here is shown schematically in Figure 1.

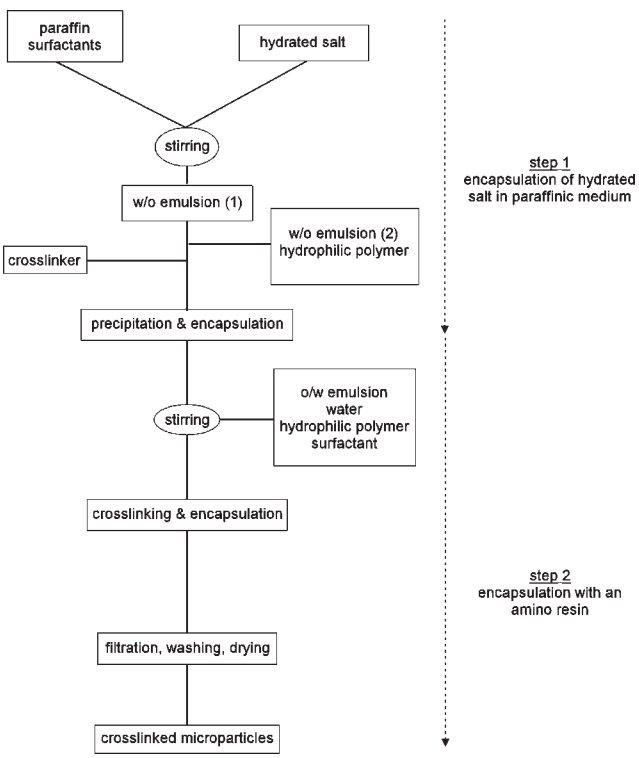

Figure 1 Schematic representation of the microencapsulation process.

Encapsulation of paraffin/microspheres by an amino-resin

The previous mixture was emulsioned in an aqueous solution containing 4 g of Tween® 20 in 100 g of water and in 9.2 g of amino resin (Arkofix NM). The pH was reduced to 3 by adding acid citric solution (30 wt %), at a stirring rate of 8000 rpm at room temperature with an homogenizer. After 3 min, the reaction mixture was heated at 60°C, whereas stirring was continued using a blade stirrer at low speed (400 rpm, RW20, IKA, Germany) for 4 h until the end of the polycondensation. Finally the microcapsules were recovered by filtration, washed with methanol and water, and dried at room temperature during one night.

Analytical methods

Interfacial tensions between the PVA-MDI microparticles and the various liquids (e.g., water, diiodomethane, *n*-hexadecane and continuous phase of the step 2) were determined by measuring the contact angle (θ) of each liquid against a disk (10^9 Pa, 14 mm in diameter) of PVA-MDI microparticles obtained by compression at room temperature of the powder. The contact angles are estimated with a goniometer equipped with a special optical system and a camera. A droplet of liquid is placed on a polymer film and the image is immediately sent via the camera to the computer for analysis. The volume of a single droplet is about 6 μL. At least four measurements were made for each liquid and mean contact angle was used to calculate the solid–liquid interfacial tension. The polar and dispersive contributions to the surface tension of PVA-MDI microparticles were calculated according to the method of Owens and Wendt[15] with water and diiodomethane.

Surface tensions of the various liquids and the interfacial tension between hexadecane and continuous phase (water and water + amino resin + Tween 20) were performed at 20°C by a ring tensiometer (Prolabo TD 2000 tensiometer) according to the ASTM C1331 and D0971, respectively. The vessel was washed with detergent, placed in chromosulfuric acid overnight, washed with distilled water, and briefly flamed with a Bunsen burner prior to use. The platinum ring was rinsed in acetone and distilled water, and flame before use. The Zuidema-Waters method was employed for the ring correction.[16]

The microscopy analyses were performed using a scanning electron microscope (Philips XL30 ESEM/EDAX-SAPPHIRE). The samples were prepared in a phenol solution to break the outer shell, EDAX being used to confirm the presence of salt in these particles.

Samples were ground and mixed with KBr to make pellets. FTIR spectra in the transmission mode were recorded using a Nicolet Nexus, connected to a PC, whose scan number was 32 and resolution 4 cm^{-1}.

The thermal behavior of hexadecane and the particles was recorded using a TA instrument type DSC 2920 piloted on PC with TA Advantage control software. Indium was used as standard for temperature calibration and the analysis was made under a constant stream of nitrogen. Samples were placed in aluminum pans, which were hermetically sealed before being placed on the calorimeter thermocouples. The sample space was purged with nitrogen at a constant flow (50 mL/min) during the experiments. Transition temperatures and enthalpies were obtained from a least four independent experiments on (4.0±)-mg samples with a scanning speed of 10 $K \cdot min^{-1}$.

RESULTS AND DISCUSSION

Step 1: Encapsulation of salt by PVA-MDI polymeric coating

Salt/hexadecane emulsion

In this part, we suggest to use a procedure based on a phase coacervation for the preparation of microcapsules from an aqueous solution of sodium phosphate dodecahydrate. Emulsion of hydrated salt in hexadecane can easily be formulated with the hydrophilic-lipophilic balance (HLB) concept of Griffin. An emulsion of very small droplets can be stable against Ostwald ripening and coalescence only by adding an appropriate surfactant. Indeed, the formation of microcapsules is greatly affected by the emulsifier, which influences not only the size but also the stability and the dispersion of microcapsules. So the emulsifiers used in the system have two functions: first, they reduce the interfacial tension between oil and aqueous phase so that smaller microcapsules can be obtained; secondly, they adsorb the water-oil interface to form a layer around the aqueous droplets to prevent their coalescence.

The surfactants used were mixtures of Span® 85 and PEG 400 dioleate in different proportions to result in HLB values covering the range 2–8. The results in Table I show that the type of emulsion and the size of the droplets differed according to the magnitude of the HLB value of the surfactants mixture. In the majority of cases, a water in oil emulsion more or less well defined is obtained, with an optimal average droplet size for a HLB value of 5–6. Furthermore, for HLB values between 5 and 7, the particles have an average diameter smaller than 1 μm.

PVA/hexadecane emulsion

The aim of this experimental part is to determine the optimum PVA concentration to obtain submicronic particles in hexadecane. The mean size of the drop-

lets in a liquid–liquid dispersion is determined by the balance between the turbulent forces tending to break up the droplets, the interfacial tension and the viscosity forces maintaining the droplet cohesion.[17] The interfacial tension of the oil/water system will depend on the temperature, the type and the concentration of PVA.[18–20] The measurements obtained by the Nouy method show that below 0.1 wt % of PVA, the interfacial tension does not vary. When the concentration is between 0.1 and 1 wt %, the interfacial tension decreases in a logarithmic way to reach a limit value (0.6 mN/m at 1 wt %). For higher concentration values (between 1 and 10 wt %), the interfacial energy is almost always constant.

Viscosity ratio measurements between PVA (in the concentration range of 1–10 wt %) and hexadecane at 20°C vary from 0.3 to 3.2. The miscroscopic observations of PVA emulsions have showed that submicronic particles are obtained for PVA concentrations at 5%, meaning a viscosity ratio close to 1 corresponding to the optimum concentration used in the process.

Micro gel creation

When the two emulsions are mixed together, the PVA droplets go closer to the salt droplets and the modification of the salt forces within the PVA particles allow their coacervation. Indeed, the salinity decreases the PVA chain solvatation in the aqueous medium, allowing the gel droplet creation due to the salting out effect. The mechanism is linked to the fact that the monomer units first start interacting with the nearest neighbors on the same PVA polymer chain during the formation of polymer aggregates in the droplet. Thus, when emulsions 1 and 2 are mixed together, a complexation reaction with the electrolyte takes place at the droplets surfaces of the w/o emulsion 2 rather than on those of the emulsion 1, because diffusing the polymeric chains to reaction sites is more difficult than transporting the low molecular complexation agent molecules. Therefore, the particle size distribution could be more affected by the viscous shearing forces than by the complexation reaction. This is why the shearing and the surfactant concentration play a major role in the encapsulation. The coacervation of salt is more efficient when emulsion 1 droplets have the same size distribution as the one of the droplets of emulsion 2 when mixed together.

Microgel crosslinking by the addition of the isocyanate

After the microgel creation, to prevent any coalescence or aggregation phenomena, the microgel particles are kept in suspension by mechanical agitation.

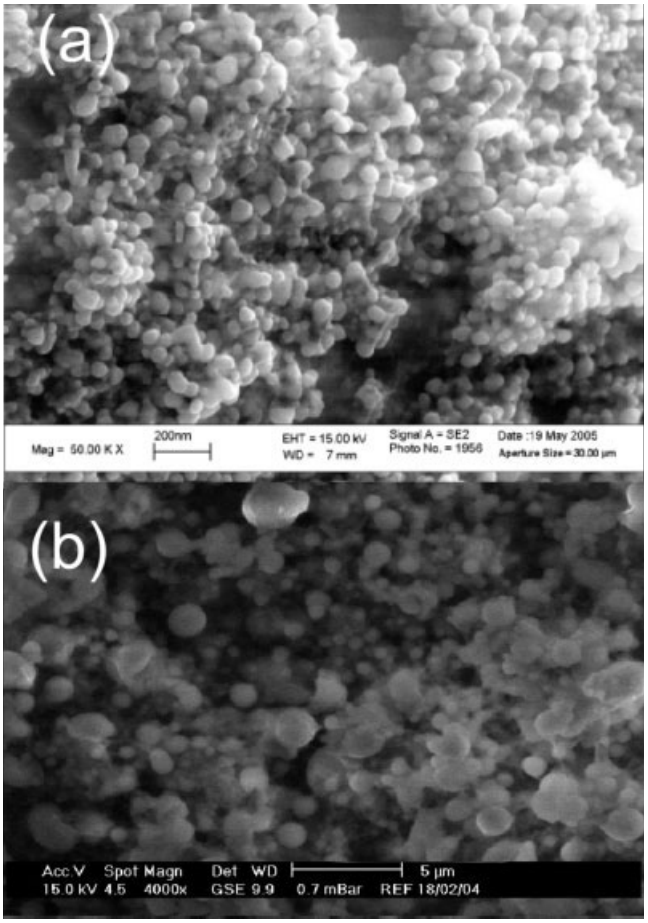

Figure 2 SEM micrographs of the PVA-MDI particles after recovery (a) and in a paraffinic medium (b).

The addition of MDI to crosslink the PVA network allows obtaining some tougher microcapsules (Fig. 2). The crosslinking reaction between PVA and MDI is very fast and has been also investigated by FTIR spectrometry (Fig. 3). The chemical schematic is showed in Figure 4. It appears that the isocyanate has reacted with the OH sites of the PVA and also with the water that was captured by the physical gel.

The infra-red spectrum of disodium hydrogen phosphate is also shown in Figure 3. In the stretching mode region of the water molecules and phosphate ions, the spectrum presents a complex absorption from 2800 and 3600 cm^{-1} due to superposition of the O—H stretching of water and PO—H groups associated through H-bonds of various strengths. Between 2500 and 1750 cm^{-1}, several weak peaks are observed and can be attributed to overtone or combination of H-bonding sensitive fundamental vibrations. The OH bending δ_{HOH} gives a sharp band at 1620 cm^{-1}. Monoprotoned (HPO_4^{2-}) species have characterized by their three absorption bands at 1073, 985, and 866 cm^{-1} corresponding to the various P—O(H) stretching vibrations, ν_{as}(P—O), ν_s(P—O) and ν(P—OH), respectively. Furthermore,

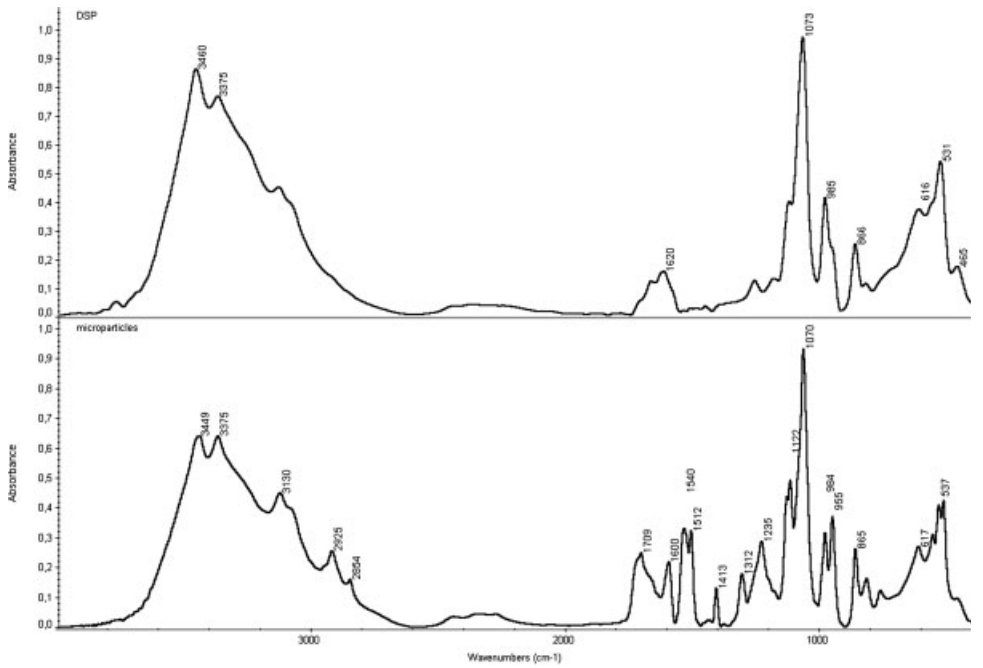

Figure 3 FTIR spectra of salt/PVA-MDI particles.

less intense broad band can be attributed to bending modes, δ(O—P—O), between 465 and 700 cm^{-1}.

The FTIR spectrum of the synthesized microcapsules presented in Figure 3 shows a doublet bands at 3450–3375 cm^{-1} that can be associated with the NH stretching modes of the free and the hydrogen bonded NH groups of the polyurethane, respectively, inside overlapped with the broad OH band. C—H stretching vibration of aliphatic methylene groups of PVA (and MDI) are shown at 2924 and 2846 cm^{-1}, respectively. The spectrum also indicated the completion of polycondensation reaction between MDI and PVA by the absence of absorption band due to isocyanate group at 2270 cm^{-1} and appearance of the C=O vibration between 1770 and 1600 cm^{-1}. N—H bending and C—N stretching at 1536 and 1234 cm^{-1}, and C—O—C stretching at 1120 cm^{-1} are also observed.

Furthermore, the spectrum shows in the carbonyl region a fairly sharp peak with a maximum at 1710 cm^{-1} and two shoulders, a broad at 1680 cm^{-1} and a thin at 1730 cm^{-1}. They could be assigned to the C=O stretching of free and bonded urea and urethane groups, respectively. The scheme reaction of urea formation is shown in Figure 5.

FTIR spectrum of microcapsules also contains characteristics absorption bands of MDI at 1598, 14,013, and 820 cm^{-1} assigned, respectively, to C=C stretching, C—C stretching and C—H bending in aromatic groups. Furthermore, the spectrum clearly

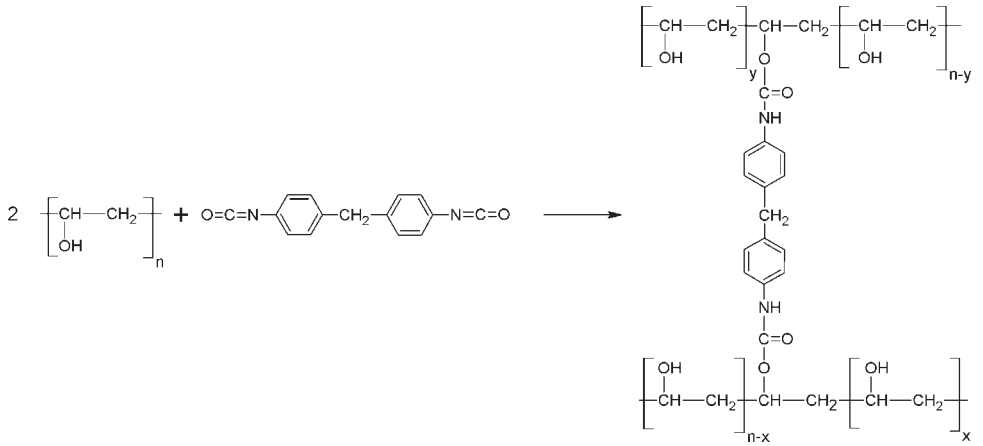

Figure 4 The reaction scheme of PVA and MDI.

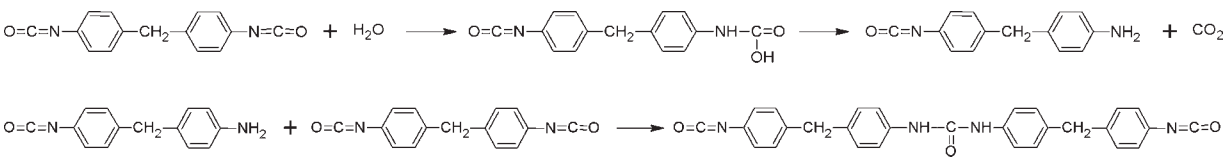

Figure 5 The reaction scheme of MDI and water.

shows that DSP was successfully microencapsulated, as it results from the presence of the characteristic three absorption bands at 1071, 984, and 866 cm^{-1} phosphate stretching vibrations.

From 1.7 up to 74 mol % of reacted hydroxyl groups of the PVA can react to crosslink with the methylene diisocyanate to achieve the reaction.[21] Nevertheless, the existence of a competitive action of at least three factors during the crosslinking—the weakening of the existing physical network due to hydrogen bonding, the formation of a chemical network, and the introduction of flexible moieties contributes to obtain homogeneous spherical structures with a smooth surface shell. A representative SEM photograph of the intermediate product prepared by the present method is shown in Figure 2(a), which illustrates the great number of entities and the uniformity in size distribution with an average diameter of $\sim$ 50 nm. Nevertheless, when they are in a paraffinic medium, they tend to agglomerate in a microsphere of a mean diameter ranging from 0.5 to 2 μm coated with paraffin [Fig. 2(b)]. Thus, the core and the shell of the particles obtained are composed of PVA crosslinked with MDI.

Step 2: Encapsulation by an aminoplast shell

Capsule formation mechanism

Multinuclear microparticles containing hexadecane and microspheres were synthesized via the *in situ* polymerization method using melamine-formaldehyde as the shell material. The ability of amino resins for self condensation around the core material droplet is linked to its surface activity and is an enrichment of resin molecules within the interface (Fig. 6). The concentration of reactive resin molecules in the boundary layer is enhanced by hydrophilic/hydrophobic interactions of the partial methylolated melamine. Thus, the resin condensation proceeds much faster in the boundary layer than in the volume phase, allowing the formation of tougher capsule walls.[22]

The morphology parameters can be separated in two categories: thermodynamic and kinetic factors. The thermodynamic factor determines the equilibrium morphology of the final particles, while the kinetic factor determines the existence ability of these morphologies. The kinetics is governed by the ability of the amino resin to self condense around the droplets. This phase is divided in two steps: preparation of stable emulsions and an *in situ* polymerization.

The determining step during a classical microencapsulation process is the emulsion. The double emulsions (w/o/w or o/w/o) are complex systems, in which the dispersed phase consists in small droplets whose composition can be similar or different to the continuous phase. However, these systems remain thermodynamically not stable and present a high trend to coalescence, creaming, and flocculation. So in this study, the main difficulty is to stabilize oil in water emulsion, with solid particles main-

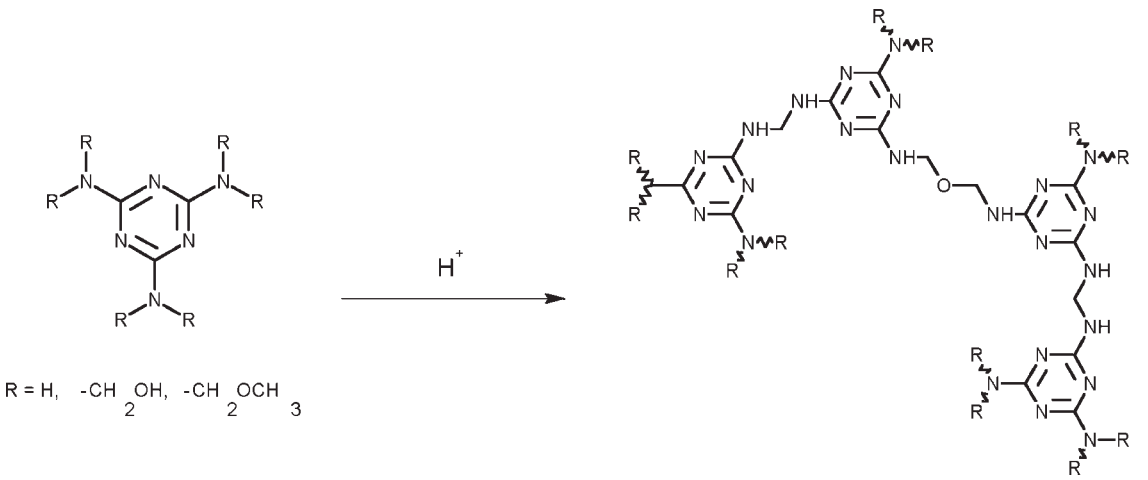

Figure 6 Formation of crosslinked amino resin shell.

TABLE II
Measured Contact Angle of the Probe Liquids and Calculated Surface Tensions by the Owens-Wendt Method[15,a]

	Mean Contact angle (θ)		Surface tension ($mN \cdot m^{-1}$)		
	Probe liquids				
Surface material	Water	Diiodomethane	γ	γ^d	γ^p
PVA-MDI	67 ± 1.1	30 ± 0.9	48.2	39.2	9
Arkofix NM	68.70 ± 1.8	41.9 ± 1.1	42.6	32.0	10.6

[a] γ, total surface energy of the surface; γ^d, dispersive component of solid surface; γ^p, polar component of solid surface.

tained in suspension by shearing the organic phase during the encapsulation with Arkofix NM.

The results of the surface and interfacial tension measurement are presented in Tables II and III, with the calculated work of adhesion and spreading coefficient. Spreading coefficients can be used to predict the engulfment of one phase within another in a third immiscible phase. Calculation of spreading coefficients, between the different interfaces present requires the knowledge of surface and interfacial tension determined either from the measurement of contact angle or Du Nouy ring method. During the contact angle measurement, the hexadecane drops spread spontaneously on the PVA-MDI and the amino resin film to such an extent that an accurate measurement of θ could not made. Thus, the interfacial tension between PVA-MDI/hexadecane and amino resin/hexadecane were calculated from the harmonic mean equation of Wu:[23]

$$\gamma_{A-B} = \gamma_A + \gamma_B - 4\frac{\gamma_A^d \gamma_B^d}{\gamma_A^d + \gamma_B^d} - 4\frac{\gamma_A^p \gamma_B^p}{\gamma_A^p + \gamma_B^p}$$

where, γ_{AB}, γ_A and γ_B are interfacial and surface tensions of the two materials in contact, respectively, and *d* and *p* superscripts represent the dispersive and the polar components of the surface tensions. For the calculation of the spreading coefficients in solution, the method of Torza and Mason was applied.

The resulting interfacial characteristics for the possible pairs are given in Table III. The entrapment depends on the spreading behavior of the hexadecane and continuous phase on the particle surface. From these results, the interfacial tension between PVA-MDI particles and hexadecane is by 15.8 $mN \cdot m^{-1}$ larger than the respective value for the pair PVA-MDI/continuous phase. This reveals a larger affinity of the PVA-MDI particles for the hexadecane phase than the aqueous medium. The lowest free energy was found for the interface between hexadecane and continuous phase. Therefore, the calculated spreading coefficients between continuous phase and solid PVA-MDI particles were negative whereas they were positive for the PVA-MDI/hexadecane interface. The calculated work of adhesion reveals stronger interaction between PVA-MDI microparticles and hexadecane than between PVA-MDI and continuous phase. According to these calculations hexadecane tends to encapsulate the PVA-MDI particles.

This quantitative analysis explains our experimental findings and more specially the morphology of the microcapsules shown in Figure 7. The particles have an occluded morphology as predicted from the spreading coefficient analysis. The core has been composed by a mixture of hexadecane and PVA-MDI microparticles entrapped by an amino resin shell. The fact that microcapsules contained in their core PVA-MDI is also illustrated in Figure 7. Large capsules have been ruptured under mechanical

TABLE III
Characteristics of Different Interfaces Present in the Microencapsulation Medium in the Emulsion Step

	Interfacial tension ($mN \cdot m^{-1}$)	Work of adhesion ($mN \cdot m^{-1}$)	Spreading coefficient ($mN \cdot m^{-1}$)[d]
Interfaces	γ_{sl}	W_a	S_i
PVA-MDI/Hexadecane	11.0[a]	64.8	11.6
PVA-MDI/Continuous phase	26.8[b]	58.9	−20.0
Hexadecane/Continuous phase	4.2[c]	60.9	−33.6

[a] Determined with the harmonic mean equation of Wu.[23]
[b] Calculated from the mean contact angle using Young's equation: $\gamma_{sv} = \gamma_{sl} + \gamma_{lv} \cos\theta$, with $\theta = 57.1 \pm 1$.
[c] Measured by the Du Nouy ring method.
[d] Calculated using the following equation: $S_i = \gamma_{jk} - (\gamma_{ij} + \gamma_{ik})$, where γ_{jk} is the interfacial tension between the phases j and k.

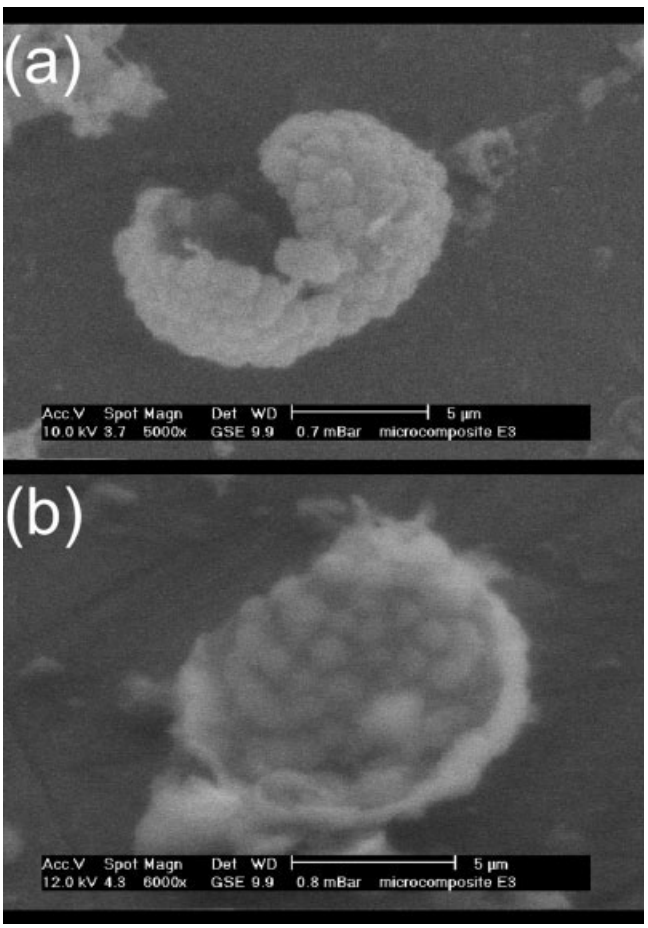

Figure 7 SEM micrographs of multinuclear microcapsules after breaking in phenol solution (outer shell and inner shell).

stress with the addition of phenol solution to weaken the shells. The SEM pictures after breakage shows the resulting hybrid structure with the presence of small spheres of ~ 1 µm in a bigger sphere. The external aspect of the particles shows an irregular and granular shell. Furthermore, the outer inner shell seems to be constituted of PVA-MDI microparticles linked together by the amino resin. We can suppose that the spreading coefficient is affected with time as the microcapsules harden, i.e., as the crosslinking reactions of melamine reins occur in the continuous phase. The polymer solution concentrations change, altering the effective surface and interfacial tensions. An indirect estimation of the final configuration can be made with the surface tension components of the amino resin film (Table II). On the one hand, the polarities of PVA-MDI and amino resin and their polar components are close and much higher than that of hexadecane. On the other hand, on the basis of the data from the Table II, the interfacial tension calculated of amino resin/hexadecane was 12.7 $mN \cdot m^{-1}$, i.e., much higher than PVA-MDI/hexadecane one. Therefore, hexadecane has much affinity with the PVA-MDI microparticles, and these latter can remain at the interface until the formation of the resin shells. Thus PVA-MDI particles tend to locate at the interface between hexadecane and amino resin, and either are linked in the inner shell or dispersed in the paraffinic medium.

Phase change properties of multinuclear microparticles

The melting behaviors of PCMs is described according two parameters, melting enthalpy corresponding to the encapsulated ratio and phase changing temperatures (i.e., the temperature of onset (T_{onset}), the temperature of the offset (T_{offset}) and the peak temperature), which can be determined by means of DSC analysis. The thermal properties of microencapsulated PCMs are strongly depend on encapsulated ratio of PCM and the chemical composition of the microcapsules shell.

Figure 8 shows the melting temperature range for hexadecane, the basic microcapsules (hexadecane encapsulated with Arkofix NM) and the multinuclear microparticles. The basic microcapsules were prepared according the process as described in the step 2. From this figure, the latent heat storage density (174 J/g) for the multinuclear particles is a little different than the encapsulated hexadecane (180 J/g) but becomes smaller than the raw material, hexadecane (227 J/g). Decrease in the melting enthalpy may be attributable to the increase in the weight due to Arkofix NM for hexadecane encapsulated and PVA/MDI/Arkofix NM for the multinuclear particles.

The DSC curves show also the onset and offset phase change temperatures, which are found to be 17.72 and 26.26°C for hexadecane, 16.57 and 28.62°C

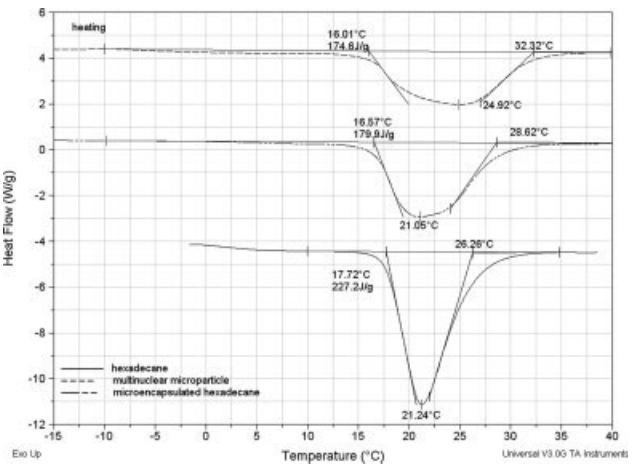

Figure 8 DSC curves for hexadecane, microencapsulated hexadecane, and multinuclear microparticles.

for microcapsules and 16.01 and 32.32°C for multinuclear microparticles, respectively. Furthermore, the phase change temperature spans ΔT (with $\Delta T = T_{offset} - T_{onset}$) are different for the different compounds. It seems that the thermal conductivity of the shell influences the heat transfer through the capsules and therefore the temperature span. Thus the incorporation of tiny PVA/MDI particles in the phase change capsules contributes to enlarge the melting range and therefore to improve the thermal properties of encapsulated material.

CONCLUSIONS

A new microencapsulation process of PCMs was performed, in which the synergetic behavior of organic and inorganic compounds allows to improve the thermal behavior of microencapsulated PCMs. The system is essentially based on the formation of three fine and stable emulsions that promote the formation of totally hydrophobic salt/PVA-MDI submicronic spheres that can be then completely confined in the paraffinic medium during the final step of microencapsulation by a melamine formaldehyde shell. The process, using the thermodynamic behavior of each phase, leads to morphology of the resultant particles accurately predicted by the analysis of the three spreading coefficients in the system. Particles with a biphasic liquid/solid cores and polymeric shells are then produced.

References

1. Liu, X.; Niu, Z.; Xu, H.; Guo, M.; Yang, Z. Macromol Rapid Commun 2005, 26, 1002.
2. Pileni, M. P. Cryst Res Technol 1998, 33, 1155.
3. Landfester, K. Macromol Rapid Commun 2001, 22, 896.
4. Cho, J.; Kwon, A.; Cho, C. Colloid Polym Sci 2002, 280, 260.
5. Fan, Y. F.; Zhang, X. X.; Wang, X. C.; Li, J.; Zhu, Q. B. Thermochim Acta 2004, 413, 1.
6. Soto-Portas, M. L.; Argillier, J. F.; Méchin, F.; Zydowicz, N. Polym Int 2003, 52, 522.
7. Uddin, M. S.; Zhu, H. J.; Hawalder, M. N. A. Int J Sol Energy 2002, 22, 105.
8. Yamagishi, Y.; Takeuchi, H.; Pyatenko, A. T.; Kayukawa, N. AIChE J 1999, 45, 696.
9. Yoshizawa, H.; Kamio, E.; Hirabayashi, N.; Jacobson, J.; Kitamura, Y. J Microencapsul 2004, 21, 2341.
10. Zhang, X.; Tao, X.; Yick, K.; Wang, X. Colloid Polym Sci 2004, 282, 330.
11. Torza, S.; Mason, S. G. J Colloid Interface Sci 1970, 33, 67.
12. Sundberg, E.; Sundberg, D. J Appl Polym Sci 1993, 47, 1277.
13. Loxley, A.; Vincent, B. J Colloid Interface Sci 1998, 208, 49.
14. Landfester, K.; Bechthold, N.; Tiarks, F.; Antonietti, M. Macromolecules 1999, 32, 5222.
15. Owens, D. K.; Wendt, R. C. J Appl Polym Sci 1969, 13, 1741.
16. Zuidema, H.; Waters, G. Ind Eng Chem 1941, 13, 312.
17. Maa, Y. F.; Hsu, C. J Controlled Release 1996, 38, 216.
18. Chatzi, E. G.; Kiparissides, C. Chem Eng Sci 1994, 49, 5039.
19. Bachtsi, A. R.; Boutris, C. J.; Kiparissides, C. J Appl Polym Sci 1996, 60, 9.
20. Yeom, C. K.; Oh, S. B.; Rhim, J. W.; Lee, J. M. J Appl Polym Sci 2000, 78, 1645.
21. Krumova, M. Polymer 2000, 41, 9265.
22. Dietrich, K.; Herma, H.; Nastke, R.; Bonatz, E.; Teige, W. Acta Polym 1989, 40, 4.
23. Wu, S. Polym Eng Sci 1987, 27, 335.